

hep-th/0304241

H I P -2003-28/TH

CERN -T H /2003-097

April 28, 2003

The Tam ing of C losed T im e-like C urves

R ahul Biswas³, Esko KeskiVakkuri^{1y}, Robert G . Leigh^{2;3z},
 Sean Nowling^{3x} and Eric Sharpe^{3{}

¹H elsin ki Institute of P hysics
 P . O . Box 9, F IN -00014 U niversity of H elsin ki, F inland

²CERN -T heory D ivision
 C H -1211, G eneva 23, S witzerland

³D epartment of P hysics, U niversity of Illinois
 1110 W . G reen Street, Urbana, IL 61801, U .S .A .

A bstract

We formulate QFT on a $R^{1,3} = Z_2$ orbifold, in a manner which is invariant under the Z_2 time and space reversal. This is a background with closed time-like curves. It is also relevant for the elliptic interpretation of de Sitter space. We calculate the one-loop vacuum expectation value of the stress tensor in the invariant QFT, and show that it does not diverge at the boundary of the region of closed time-like curves. Rather, the only divergence is at the initial time slice of the orbifold, analogous to a spacelike Big Bang singularity. We then calculate the one-loop graviton tadpole in bosonic string theory, and show that the answer is the same as if the target space would be just the Minkowski space $R^{1,3}$, suggesting that the tadpole vanishes for the superstring. Finally, we argue that it is possible to define local S-matrices, even if the spacetime is globally time-nonorientable.

E-mail: rbiswas@students.uiuc.edu

^yE-mail: esko.keski-vakkuri@helsinki.fi

^zE-mail: rgleigh@uiuc.edu

^xE-mail: nowling@students.uiuc.edu

[{]E-mail: ersharp@uiuc.edu

1 Introduction and Summary

A technical obstacle in exploring string theory in time-dependent spacetimes is to find suitable backgrounds where string quantization is tractable. Early work includes [1, 2, 3, 4, 5, 6]. More recently, interest has been revitalized, motivated in part by novel string-based cosmological scenarios (see for example [7, 8, 9]). An obvious path to follow was to construct such backgrounds as time-dependent orbifolds of Minkowski space [10, 11, 12, 13, 14, 15, 16, 17, 18] or anti-de Sitter space [19, 20, 21]. Further related work includes [22, 23, 24, 25, 26, 27, 28, 29, 30, 31, 32]. However, depending on how the orbifold identifications are defined, potentially dangerous issues may arise. The resulting time-dependent orbifolds can have regions with closed time-like curves (CTCs) or closed null curves (CNCs), or may not even be globally time-orientable. Therefore, one could choose to first make a list of desirable features for the orbifolds and then try to limit the study only to those backgrounds that possess those features. This sensible strategy was laid out and pursued by Liu, Moore and Seiberg [14, 15]. For orbifolds of type $R^{1,3}/\Gamma$ where Γ is a discrete subgroup of the Poincare group, the list turned out to be very short containing only the null branes with $R > 0$. However, the null brane construction involves identifications by arbitrarily large boosts. This turns out to be another potential reason for instabilities, and it was argued by Horowitz and Polchinski [16] that such backgrounds become unstable after just a single particle is added, because on the covering space the particle can approach its initiality many times with increasingly high momenta and produce a black hole. Additional discussion of potential problems can be found in [17, 15, 26].

Aside from constructing and studying time-dependent backgrounds by alternative methods, one might speculate if the list of desirable features for suitable orbifold backgrounds was too prohibitive and reconsider the reasons for including each item on the list. In any case, it is important to understand if and/or why string theory actually has problems with these features. The reason for demanding that there be no regions containing closed time-like curves appears obvious. CTCs violate causality, and it has been conjectured by Hawking [33] that the laws of physics prevent CTCs from appearing. The arguments in support of this chronology protection conjecture (CPC) are usually based on general relativity plus matter at the classical or semi-classical level. A recent summary can be found in [34]. Essential features are that perturbations can keep propagating around a CTC so that backreaction accumulates, or quantum effects can lead the matter stress tensor to diverge at the boundary of the CTC region, leading to infinite backreaction. However, the trouble with CTCs and CNCs seems to arise from propagation along them, rather than merely from their existence. It is not clear if the two are equivalent. For example, the model studied in [10] involves CTCs and CNCs, but it was argued that they

do not necessarily pose a problem in quantum mechanics if one projects to a subspace of states which do not time evolve along the CTCs and CNCs. Another desirable feature on the list was time-orientability. This was included to avoid problems in defining an S-matrix, and problems associated with the existence of spinors [35, 36, 37]. However, the consequences of a lack of time-orientability have not yet been subject to extensive investigation and are thus less well understood. From the point of view of local physics, one might wonder if the whole Universe could be globally time-nonorientable, but in such a way that the global feature could only be detected by meta-observers and never be revealed by local experiments. The orbifold studied in [10] is an example of a spacetime which is globally time-nonorientable. In any case, its structure appears to allow for a definition of an S-matrix for local experiments.

To summarize, there are many reasons to investigate the chronology protection conjecture and time-nonorientability. We also note that recently the former topic has been investigated from other points of view in the context of string theory and holography [38, 39, 40, 41, 42].

The R^{1+1}/Z_2 orbifold, obtained by identifying points X with reflected points $-X$, provides a simple model which incorporates both issues. Some comments were made in passing in [10]. In this paper we perform a more detailed investigation. First, we formulate quantum field theory in a manner which appropriately incorporates the Z_2 identification under time reversal and space reflection. This construction is also relevant for the elliptic interpretation of de Sitter space (dS) [43, 44, 45, 46]. A d -dimensional de Sitter space is a time-like hyperboloid embedded in R^{1+1} . The Z_2 reflection on R^{1+1} induces an antipodal reflection on the dS spacetime. The elliptic de Sitter space dS/Z_2 is then defined by identifying the reflected antipodal points. Previous studies of the elliptic dS spacetime have discussed problems in defining a global Fock space in the global patch; however, it was possible to construct QFT and a Fock space by restricting to the static patches of observers at the (identified) north and south poles. Similar problems are encountered in trying to formulate QFT on R^{1+1}/Z_2 . We circumvent these problems by first doubling the field degrees of freedom, with the copy fields propagating towards the reversed time direction, and then identifying the degrees of freedom under the Z_2 reflection. The doubling of fields is motivated by (the zero temperature limit of) the real-time formulation of finite temperature QFT. The doubling of degrees of freedom helps to overcome problems with causality when the light-cones of the identified points X and $-X$ intersect, as we will assume that the two copies of the fields (at X and $-X$) are dynamically decoupled. Note that in the limit in which the cosmological constant approaches zero, the dS spacetime becomes locally Minkowski spacetime. Correspondingly, it has been argued that in this limit the elliptic dS spacetime goes to two copies of Minkowski spacetime, related by the Z_2 reflection [46]. In the present work, we would instead propose that QFT on the elliptic

ds spacetime goes to QFT on $R^{1+d} = \mathbb{Z}_2$, with two copies of fields, identified under the \mathbb{Z}_2 refection.

After introducing the \mathbb{Z}_2 invariant QFT, we show that the reformulation of QFT removes the infinite backreaction normally associated with the boundary of the CTC region. This is not necessarily a contradiction with the CPC, since the reformulation can also forbid propagation around a CTC. We then study the backreaction at one-loop level in string theory. We calculate the one-loop graviton tadpole in the $R^{1+d} = \mathbb{Z}_2$ background, and show that the answer is the same as if the background were just R^{1+d} ! While the answer by itself would at first appear puzzling, it appears very natural in relation to the \mathbb{Z}_2 invariant formulation of QFT. Indeed, the low-energy limit of string theory should be the \mathbb{Z}_2 invariant QFT. Finally, we argue that it is possible to define S -matrices in a manner that makes sense locally. The definition only breaks down at the point which can be regarded as the initial "Big Bang singularity" of the orbifold, and at that point we also find that even in the invariant reformulation of the QFT, the stress tensor diverges. However, it is also possible that stringy effects lead to a smooth blow-up of the orbifold singularity. Then the QFT would need to be reconsidered in this smooth background.

We have organized the paper as follows. In Section 2, we review some features of the time-dependent orbifold background, and focus on some novel features of these orbifolds. In particular, we point out that a choice of time orientation must be made. In Section 3, we review the (naive) analysis of the gravitational back reaction in this geometry. In Section 4, we present a proper formulation of quantum field theory on the $R^{1+d} = \mathbb{Z}_2$ background, and show that the only divergence of the stress tensor, beyond the familiar short-distance Minkowski spacetime divergence, can be interpreted as a "cosmological initial condition." In Section 5, we present some details of similar calculations in string theory which demonstrate the same results (complementary calculations in a different formalism are shown in the Appendix.) Finally, in Section 6, we discuss further features of the interacting QFT, including a discussion of the S -matrix.

2 Overview of $R^{1+d} = \mathbb{Z}_2$

Let us first review some features of the $R^{1+d} = \mathbb{Z}_2$ orbifold [10]. We begin with the covering space R^{1+d} and identify the time and space coordinates under the refection

$$(t; x^a) \rightarrow (t; -x^a) : \quad (1)$$

The resulting orbifold is a space-time cone, depicted in Figure 1 for $d = 1$. Points in the opposite quadrants are identified. The orbifold contains closed time-like curves, an example of which is depicted in the figure. Orbifolds that act purely spatially are familiar

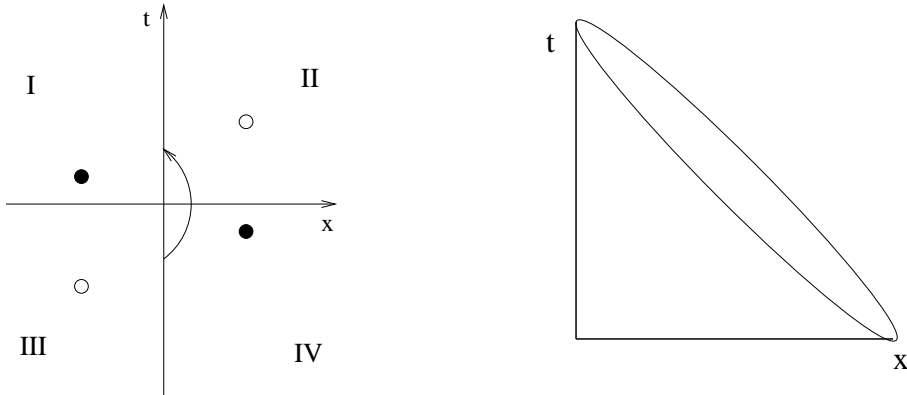


Figure 1: The orbifold $R^{1,1}/Z_2$.

and are certainly well understood. New problems arise when the identification involves the time direction; for example it is not guaranteed that the string spectrum will be free from tachyons and ghosts. Ref. [10] investigated bosonic and type II superstrings on $R^{1,1}/Z_2 \times R^n$, with n additional spacelike directions added to bring the total spacetime dimension to 26 or 10. It was shown, using a Euclidean continuation, that although the background is time-dependent and quantization had to be done in the covariant gauge, the physical spectrum did not contain any negative norm states (ghosts). The superstring spectrum did not contain any tachyons. Also, the one-loop partition function vanishes for the superstring.

Although string theory passed the first tests, questions associated with the time identification on the orbifold remained. In the orbifold (1), there is actually extra data that must be specified. To see this, we note that to specify a Lorentzian metric on an orientable space M ($w_1(M) = 0$), we must specify a time orientation. Mathematically, this implies a real rank 1 subbundle $L \subset TM$, the time orientation bundle. M is said to be globally time-orientable when $w_1(L) = 0$.) A time-like Killing vector defining time's arrow, if available, would be a global section of this line bundle.

In the case of the orbifold (1), we must ask how various quantities descend from the covering space to the orbifold. In particular, $\theta = \theta t$ is manifestly not invariant under the group action, and so does not define a time's arrow, or time-like Killing vector, in the quotient. Thus, this orbifold leaves ambiguous the direction on which time flows in the quotient (we must manually make a choice of direction of time-flow).

Furthermore, the natural time orientation bundle on the covering space does descend to the quotient space, but (omitting the singularity at the origin) the class $w_1(L)$ is non-trivial. Thus the image of L on the quotient is not time-orientable. Although locally we can choose a perfectly sensible notion of time orientation, this is not possible globally.

In fact, there are essentially three choices. To illustrate, let us consider the case of

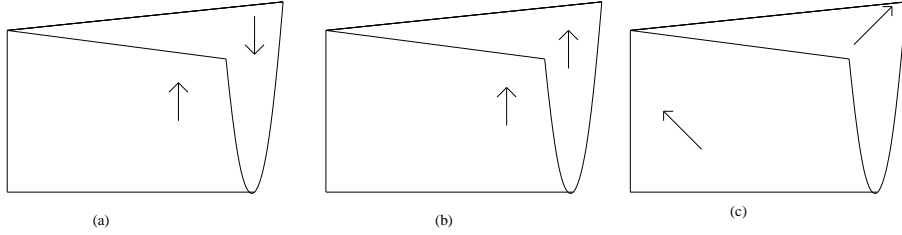


Figure 2: Three possible time-arrows on the quotient $R^{1,1}/Z_2$.

$R^{1,1}/Z_2$. The obvious choice of time's arrow on the covering space $R^{1,1}$, namely $\theta = \theta t$, is not invariant under the group action, a property which manifests itself in the observation that by picking different fundamental domains for the group action on the cover, the time's arrow in those fundamental domains restricts to a different time's arrow on the quotient.

In Fig. 2 we have shown three possible time-arrows that one can construct on $R^{1,1}/Z_2$. The left-most case corresponds to taking the fundamental domain to be regions II and IV, the middle case corresponds to taking the fundamental domain to be regions I and II, and the right-most case corresponds to taking the fundamental domain to be one side of a wall of the lightcone. In this case, omitting the origin, the time-orientation line bundle on the quotient is not orientable ($w_1(L) \neq 0$), hence each choice of time's arrow depicted in Figure 2 has zeroes (in case (a), along the left vertical crease, and in case (b), along the bottom horizontal crease). Note that in each case it would also be possible to choose a reverse time orientation (reversed arrows). Then e.g. Fig. 2(b) would depict a "big crunch".

In Figure 3, we have drawn the quotient space corresponding to Fig. 2(a). In this case, there are asymptotic regions for both $t > 1$. Another choice for the quotient space, corresponding to Fig. 2(b), is shown in Fig. 4. In this case, there is no asymptotic region corresponding to $t > 1$. Instead, we have a "big bang" singularity at $t = 0$. It is interesting to contemplate the properties of quantum field theory on such a spacetime. It is of even more interest to ponder the role of string theory. We will return to a more thorough discussion of these issues in a later section.

3 Backreaction in Quantum Field Theory

Here we give a short review of the standard QFT calculation for the vacuum expectation value (vev) of the stress tensor, showing that it diverges at the boundary of the CTC

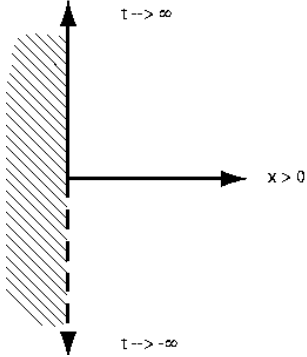


Figure 3: A view of the quotient spacetime (for 1+1 dimensions). Note the absence of the $x = 0$ axis for $t < 0$.

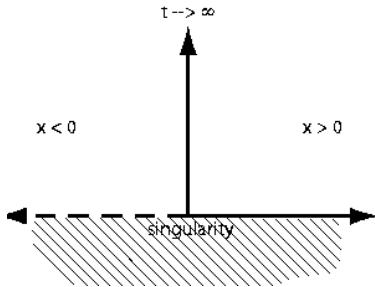


Figure 4: Another view of the quotient spacetime (for 1+1 dimensions). Note the absence of the $t = 0$ axis for $x < 0$. The $t = 0$ axis represents a 'big bang' singularity (the beginning of the spacetime).

region. Later, we will contrast this with a calculation in string theory.

The standard argument for the instability of a spacetime (here, specifically, a spacetime orbifold) with closed time-like curves proceeds as follows. The gravitational backreaction from the renormalized stress energy of a quantum field may be evaluated semi-classically

$$G = 8 G_N h T_{\text{ren}} : \quad (2)$$

Here the subscript refers to the fact that we subtract off the usual vacuum energy contribution | the curvature is well-defined if there are no divergences other than the usual at space short distance singularities. When one evaluates the right hand side, one expects to find it to diverge at the boundary of the CTC region, signaling infinite backreaction and instability of the spacetime.

The $R^{1,1}/\mathbb{Z}_2$ orbifold has a region of closed time-like curves. On the covering space, it is the region bounded by the future and past light-cones emanating from the origin. Then

one would expect that the vacuum expectation value of the stress tensor diverges on the light-cones, signaling potential instability. Indeed, a quick calculation yields just such a divergence. To illustrate the point, consider the R^{1+1}/\mathbb{Z}_2 orbifold and a free massless scalar field. The field decomposes into left- and right-moving sectors. Let us focus on the right-moving ones only. The right-moving component of the stress tensor is

$$T_{uu}(u) = : \partial_u(u) \partial_{u^0}(u) :; \quad (3)$$

where $u = t - x$. In Minkowski space, this is obtained by subtracting the divergence that is uncovered through point-splitting

$$T_{uu}(u) = \lim_{u^0!} \frac{1}{u} \partial_u(u) \partial_{u^0}(u^0)_{\text{ren}} \quad (4)$$

making use of the two-point function

$$G(u; u^0) = h_0 j(u) j(u^0)_{\text{pi}} \ln(u - u^0) : \quad (5)$$

On the orbifold, we require the field operator and the stress tensor to be invariant under the $(t; x) \mapsto (t; x) \mathbb{Z}_2$ reflection. For the right-moving component, let us impose the invariance by considering

$$\tilde{\sim}(u) = \frac{1}{2} (j(u) + j(-u)) : \quad (6)$$

The renormalized expectation value of the \mathbb{Z}_2 invariant stress tensor is then

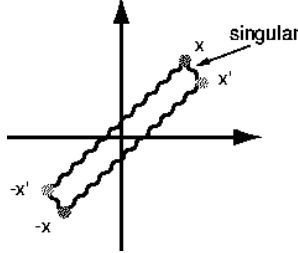


Figure 5: Correlator of point-split composite operator. The 'short' contractions, between x and x^0 are the usual short-distance ones, and should be subtracted. The 'long' contractions give rise to the Casimir energy.

$$\begin{aligned} hT_{uu}(u)_{\text{ren}} &= \lim_{u^0!} \frac{1}{u} \partial_u \partial_{u^0} h_0 j(u) + j(-u) g f(u^0) + j(-u^0) g_{\text{ren}} \\ &= \lim_{u^0!} \partial_u \partial_{u^0} f \ln(u - u^0) \ln(u + u^0) g_{\text{ren}} \\ &= \lim_{u^0!} \frac{1}{u} \frac{1}{(u + u^0)^2} = \frac{1}{4u^2} : \end{aligned} \quad (7)$$

This diverges on the null line $u = 0$, which is a part of the boundary of the CTC region. A similar calculation for the left-movers yields a divergence at the other part of the boundary, $v = 0$. Hence one concludes that the orbifold is potentially unstable. Similar calculations can be done in higher dimensions.

However, upon closer inspection the above argument has some puzzling features. The most cumbersome one is that the Z_2 invarianteld operator (6) has the mode expansion

$$\sim(u) = \frac{p_-^Z}{2} d! (a_i + a_i^Y) \cos(!u) \quad (8)$$

so it is not clear what exactly is meant by the naive notion of particles and vacuum. The problem of constructing a global Fock space is also well known from investigations of elliptic de Sitter space $dS = Z_2$ [43, 44, 45, 46]. In the above, the problem has been lifted onto $R^{1,d} = Z_2$, where the $dS = Z_2$ can be embedded.

Actually, we will argue that the orbifold identification requires identifying a particle with positive energy at $(t; x)$ with a particle with negative energy at $(-t; -x)$. Particles of the latter kind cannot be created with a_i^Y . A quick look at the mode expansion of $\sim(u)$ might give a false impression that this would happen, but really $\sim(u)$ is just theeld operator evaluated at point u rather than a new operator with the creation and annihilation operators acting in a different way. Another problem is that the usual prescription calls us to evaluate commutators ofeld operators at equal time. On the orbifold covering space this becomes problematic, since "equal time" now corresponds to times t and $-t$. For these reasons we would like to take a step back and reconsider the formulation ofeld theory on the $R^{1,d} = Z_2$ orbifold.

4 Quantum Field Theory on $R^{1,d} = Z_2$ Revisited

Consider a point particle on the fundamental domain of $R^{1,d} = Z_2$. On the covering space, it corresponds to two particles: one with positive energy (propagating forward in time), and its image with negative energy (propagating backward in time) with opposite momentum (Fig. 6). In other words, for each particle with a momentum $(k^0; \vec{k})$ we must include its image with momentum $(-k^0; -\vec{k})$.

The situation is similar for strings on $R^{1,d} = Z_2$, analyzed in [10]. The states in the untwisted sector which survive the Z_2 projection are of the type

$$j_{is} = \frac{1}{n_1} \quad \frac{1}{m_1} \sim_{S,A} (\beta; ki \quad \beta; -ki); \quad (9)$$

i.e. symmetrized combinations of string states with opposite pairs of center-of-mass momentum k . We conclude that in order to have a good description of quantum mechanics on the orbifold, we must start with pairs of states with opposite energy and momentum.

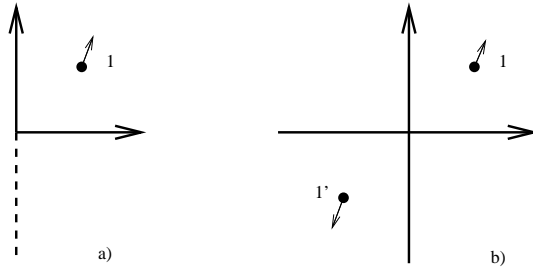


Figure 6: A point particle on the orbifold. a) depicts a single point particle on the fundamental domain, while b) depicts the point particle and its image on the covering space, moving towards the opposite time and space directions.

In quantum field theory in Minkowski space, 1-particle states in the Fock space are associated with positive energy,

$$j_{\mathbf{k};\mathbf{k}} = a_{\mathbf{k}}^{\dagger} \mathcal{D}_{\mathbf{k}} \text{ with } k^0 = \mathbf{k} > 0: \quad (10)$$

However, in order to formulate a quantum field theory on the orbifold covering space, we must also be able to include states with $k^0 = -\mathbf{k} < 0$. In other words, what we need is a Fock space H which involves sectors with both sign choices for the energy:

$$\begin{aligned} H^+ &= \bigcup_{\mathbf{k}} H_{\mathbf{k}}^+ \text{ with } k^0 = \mathbf{k} > 0 \\ H^- &= \bigcup_{\mathbf{k}} H_{\mathbf{k}}^- \text{ with } k^0 = -\mathbf{k} < 0 : \end{aligned} \quad (11)$$

The full Fock space is then the direct sum

$$H = H^+ \oplus H^- : \quad (12)$$

In order to construct an invariant Fock space on the orbifold, we need to first implement the Z_2 action as an isomorphism $H \rightarrow H$ which acts by inverting the sign of energy and momentum in the orbifolded directions. In particular, the usual vacuum $\mathcal{D}_{\mathbf{k}} \in H^+$ must map to a state in H^- ; we will call it $\mathcal{D}_{\mathbf{k}}$. We will later define it and other states in H more precisely. The invariant Fock space is then

$$H_{\text{inv}} = H / Z_2 : \quad (13)$$

Given this orbifold identification, it should be noted that there is no particular problem with the stability of the theory related to a negative energy sea.

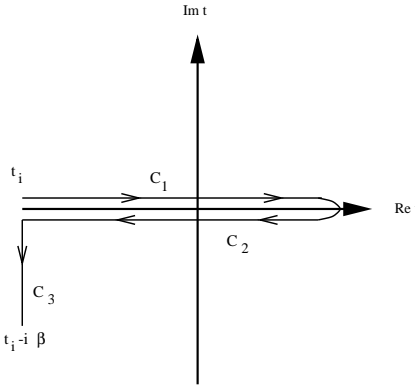


Figure 7: The time contour for FTQFT .

There are of course well known reasons to involve both positive and negative energy sectors in the formulation of QFT . One of them is QFT in curved spacetime, or other cases where we compare observers who are not related by proper orthochronous Lorentz transformations. The mode expansions of the field operator relevant for such observers are related by mixing of positive and negative energies. In the present case, the $R^{1+1} = Z_2$ spacetime is locally flat, but we want to identify (as opposed to compare) observers related by the time (and space) reflection, and identify the corresponding degrees of freedom .

Actually, a closely related starting point is QFT in flat spacetime but at finite temperature (FTQFT). The real-time formulation of FTQFT also leads to mixing between positive and negative energies. For inspiration, we shall review it briefly. The starting point in the path integral formulation of real-time FTQFT is the generating functional

$$Z[J] = \int_C d^4x \mathcal{L}(\phi(x)) + J(x)\phi(x) \quad (14)$$

where the time integral has been promoted to a contour integral along a complex time path C , starting from some initial time t_i and ending at a complex final time $t_f - i\beta$, where the imaginary part is given by the inverse temperature $\beta = T^{-1}$ [47]. The functional integral is taken over all field configurations which satisfy the periodic boundary condition

$$\phi(t_i - i\beta; x) = \phi(t_f; x) : \quad (15)$$

One convenient choice of the complex time path consists of three segments, $C = C_1 \cup C_2 \cup C_3$, where C_1 runs along the real axis from t_i to some $t_f - t_i$, C_2 runs backwards along the time axis from t_f to t_i , and finally C_3 runs parallel to the imaginary axis from t_i to $t_i - i\beta$ (Fig. 7).

From the generating functional, one can calculate the thermal Green's function

$$iD_C(x - x') = hT_C(x)(x')i; \quad (16)$$

where time ordering has been promoted to path ordering T_C along the complex time path C . Equivalently, one can rewrite the thermal Green's function in terms of a 3×3 matrix $(D^{rs})_{rs=1,2,3}$ with components

$$D^{rs}(t - t') = D_C(t_r - t_s) \quad (17)$$

where $t = t_r$; $t^0 = t_s$ if $t \in C_r$ and $t^0 \in C_s$ along $C = C_1 \cup C_2 \cup C_3$. Furthermore, it can be shown that if one takes $t_i, t_f \in C_1 \cup C_2$ in an appropriate manner, the contributions involving the segment C_3 decouple from the rest. The matrix (D^{rs}) then reduces to a 2×2 matrix, but the temperature dependence remains, as the components depend on the distribution function of the thermal background. The contour C reduces to the Schwinger-Keldysh contour [48, 49] $C_1 \cup C_2$. The propagator is reproduced by breaking up the field and the source J into two-component vectors,

$$\begin{aligned} &= (J_1; J_2) \text{ with } J_r(x) = (t_r; x); t_r \in C_r \\ J &= (J_1; J_2) \text{ with } J_r(x) = J(t_r; x); t_r \in C_r : \end{aligned} \quad (18)$$

The generating functional (14) then reduces to a form

$$Z[J_1; J_2] = \int D[1] D[2] \exp \left[i \int d^4x [J_r D^{-1}]^{rs} s + L_{\text{int}}(1) - L_{\text{int}}(2) + J_r J_r \right] \quad (19)$$

where L_{int} is the interaction part of the Lagrangian. In particular, the diagonal components of the 2×2 propagator D^{rs} have the momentum space representation

$$\begin{aligned} iD^{11}(k) &= \frac{i}{k^2 - m^2 + i} + 2(k^2 - m^2)n_T(k_0) \\ iD^{22}(k) &= \frac{i}{k^2 - m^2 - i} + 2(k^2 - m^2)n_T(k_0) \end{aligned} \quad (20)$$

where $n_T(k_0)$ is essentially the thermal distribution function. It is then evident that in addition to the physical field 1 , the theory contains another degree of freedom 2 , called the thermal ghost, which propagates backwards in time. The two fields $1, 2$ are coupled together only by the off-diagonal elements $D^{12, 21}$ of the propagator. One is interested in correlation functions of 1 only. Furthermore, it can be shown that in the zero temperature limit $T \rightarrow 0$ the off-diagonal elements of the propagator vanish, $D^{12, 21} \rightarrow 0$, so that the thermal ghost decouples from the physical degree of freedom. Hence at zero temperature one can ignore the thermal ghost and the theory reduces back to the usual form involving only the physical degree of freedom. But at any finite T , both fields make physical contributions.

The orbifold case. In the above example, the Fock spaces associated with the physical eld and thermal ghost are the positive and negative energy sectors H^+ and H^- . At zero temperature, before removing the thermal ghost, the generating functional (19) is symmetric under Z_2 reflection which reverses the direction of time. This is precisely what we need as a starting point for QFT on the covering space of $R^{1,3}/Z_2$. We will also start with a path integral involving the Schwinger-Keldysh contour as the complex time path. Then, as before, we break up the eld as a two-component vector $\phi = (\phi_+; \phi_-)$ where ϕ_+ and ϕ_- involve times at the forward and backward running segments of the Schwinger-Keldysh contour. The path integral can then be rewritten as

$$Z = \int_{-i\infty}^{i\infty} D\phi_+ D\phi_- \exp \left[i \int_1^{\infty} dt \, d^d x [L(\phi_+) - L(\phi_-)] \right]; \quad (21)$$

where L is the (for example) scalar eld Lagrangian

$$L(\phi) = \frac{1}{2} (\partial_\mu \phi)^2 - \frac{1}{2} m^2 \phi^2 - V_{\text{int}}(\phi); \quad (22)$$

We have made physical input here by the choice of propagator for ϕ_+ ; ϕ_- . On the covering space, our picture is that the eld ϕ_+ propagates forward and its copy eld propagates backward in time, decoupled from each other for $t \neq 0$. Hence the propagator is diagonal in ϕ_+ . We then choose the $t = 0$ hypersurface as the time slice where we define initial conditions⁶. More precisely, we could consider the time evolution of ϕ_+ from $t < 0$ up to a specified profile at $t = 0$ and then forward to $t > 0$, and the reverse for ϕ_- . The orbifold identification then calls us to identify the elds and time evolutions (elaborated further below). However, note first a subtlety in defining the initial condition. At $t = 0$ the orbifold identification is $(0; x) \leftrightarrow (0; -x)$, hence the profiles of ϕ_+ and ϕ_- must become symmetric at $t = 0$. The most natural initial condition is to set the profiles to be equal at $t = 0$. Thus our initial condition is

$$x > 0 : \phi_+(0; x) = \phi_-(0; -x) = \phi_0(x) = \phi_-(0; x) = \phi_0(x) \quad (23)$$

where $\phi_0(x)$ is the specified initial profile on $x > 0$. This can be satisfied as follows. Decompose the elds into symmetric and antisymmetric parts under $x \leftrightarrow -x$:

$$\begin{aligned} \phi(t; x) &= \phi_S(t; x) + \phi_A(t; x); \\ \phi_S(t; x) &= \frac{1}{2} (\phi_+(t; x) + \phi_-(t; -x)) \\ \phi_A(t; x) &= \frac{1}{2} (\phi_+(t; x) - \phi_-(t; -x)); \end{aligned} \quad (24)$$

⁶Hence we are choosing the fundamental domain to be that of Figures 2 b) and 4. While this is the most convenient choice for our QFT construction, other choices would also be possible.

The initial condition can be satisfied if the antisymmetric parts decay to strictly zero sufficiently rapidly as $t \rightarrow 0$ (and the symmetric parts become equal). There is a subtlety here in what exactly should be meant by "sufficiently rapid," and we will comment on it further below.

While the above serves as a starting point for our construction of the theory on the covering space, we must also take into account the identification which is part of the orbifold construction. We already discussed this in the context of Fock space states, and can now do it more explicitly. Let us leave the path integral formalism and return back to the canonical quantization prescription. In the remainder of this section, we focus only on the free field part of the Lagrangian. This is sufficient for the construction of the invariant Fock space, and for the improved invariant version of the back-reaction calculation which will replace that of Section 3. We will present a tentative discussion of interacting theory and the S-matrix in Section 6.

First, we quantize the field operators a_{\pm} . While a_+ has the standard free field mode expansion

$$a_+(t; \mathbf{x}) = \frac{Z}{(2\pi)^d} \frac{1}{\prod_{k=1}^n} a_k e^{i\omega_k t + i\mathbf{k} \cdot \mathbf{x}} + a_k^* e^{+i\omega_k t - i\mathbf{k} \cdot \mathbf{x}}^* ; \quad (25)$$

for the operator a_- we write the mode expansion as

$$a_-(t; \mathbf{x}) = \frac{Z}{(2\pi)^d} \frac{1}{\prod_{k=1}^n} a_k e^{+i\omega_k t - i\mathbf{k} \cdot \mathbf{x}} + a_k^* e^{i\omega_k t + i\mathbf{k} \cdot \mathbf{x}}^* ; \quad (26)$$

The initial condition at $t = 0$ and the required rapid decay of the antisymmetric parts of a_- create subtleties, but the above mode expansions are valid sufficiently far from the $t = 0$ slice. Since the field a_- is decoupled from a_+ , we introduced a new set of annihilation and creation operators $a_k; a_k^*$ which commute with $a_k; a_k^*$:

$$[a_k; a_{k0}^*] = [a_k^*; a_{k0}^*] = [a_k^*; a_{k0}] = [a_k^*; a_{k0}^*] = 0 ; \quad (27)$$

However, the new operators a satisfy the standard commutation relation

$$[a_k; a_{k0}^*] = (2\pi)^d \delta^{(d)}(\mathbf{k} - \mathbf{k}^0) ; \quad (28)$$

Thus, whereas a_k destroys a particle with wavefunction $e^{i\omega_k t + i\mathbf{k} \cdot \mathbf{x}}$ which is positive energy and momentum with respect to the Killing vectors $E = i\partial_t$ and $P = i\mathbf{r}$, the new annihilation operator a_k destroys a particle with wavefunction $e^{i\omega_k t - i\mathbf{k} \cdot \mathbf{x}}$ which is negative energy and opposite momentum with respect to E and P . Let us then define a new vacuum $|0\rangle$ and 1-particle states:

$$\begin{aligned} |0\rangle &: a_k |0\rangle = 0 \\ j_{-k}; \alpha_k &: j_{-k}; \alpha_k = a_k^* |0\rangle : \end{aligned} \quad (29)$$

We use the notation $j_{\vec{k}}^{\dagger}; \vec{k}i$ to emphasize that these particles carry negative energy and opposite momentum. The above states are the images of the usual vacuum and 1-particle states of H^+ under the Z_2 isomorphism $H^+ \rightarrow H^-$, that we discussed earlier.

Next we need to take into account the identification and define Z_2 invariant states on the fundamental domain; these are states in the invariant Fock space $H_{\text{inv}} = (H^+ \otimes H^-) = Z_2$. E.g. for 1-particle states we define

$$j_{\vec{k}}^{\dagger}; \vec{k}i_{\text{inv}} = \frac{1}{2} (j_{\vec{k}}^{\dagger} + \vec{k}i^{\dagger} + \vec{p}i^{\dagger} - j_{\vec{k}}^{\dagger} - \vec{k}i^{\dagger}) = \frac{1}{2} \vec{p}^{\dagger} : j_{\vec{k}}^{\dagger}; \vec{k}i : \quad (30)$$

Invariant multiparticle states are constructed in an analogous fashion. Next we define a number operator on the fundamental domain,

$$N_{\vec{k}}^{\text{inv}} = a_{\vec{k}}^{\dagger} a_{\vec{k}} \quad a_{\vec{k}}^{\dagger} a_{\vec{k}} = \begin{matrix} a_{\vec{k}}^{\dagger} a_{\vec{k}} \\ a_{\vec{k}}^{\dagger} a_{\vec{k}} \end{matrix} : \quad (31)$$

Clearly,

$$N_{\vec{k}}^{\text{inv}} j_{\vec{k}}^{\dagger}; \vec{k}i_{\text{inv}} = 1 \quad j_{\vec{k}}^{\dagger}; \vec{k}i_{\text{inv}} : \quad (32)$$

We propose that the natural energy operator on the orbifold is

$$H_{\text{inv}} = \sum_{\vec{k}} N_{\vec{k}} !_{\vec{k}} = \sum_{\vec{k}} !_{\vec{k}} a_{\vec{k}}^{\dagger} a_{\vec{k}} \quad !_{\vec{k}} a_{\vec{k}}^{\dagger} a_{\vec{k}} : \quad (33)$$

Let us compare this with the stress tensor. The action (21)

$$S = \int_1^Z dt \int d^d x [L(+)-L(-)] \quad (34)$$

yields a stress tensor (for brevity, we consider a massless scalar field)

$$\begin{aligned} T &= \frac{S}{Z} = \partial_+ \partial_- + \partial_- \partial_+ \\ &= T^+ - T^- : \end{aligned} \quad (35)$$

From T_{00} we derive the associated Hamiltonian

$$H = \frac{1}{2} \sum_{\vec{k}} !_{\vec{k}} [a_{\vec{k}}^{\dagger} a_{\vec{k}} + a_{\vec{k}} a_{\vec{k}}^{\dagger}] - \frac{1}{2} \sum_{\vec{k}} !_{\vec{k}} [a_{\vec{k}}^{\dagger} a_{\vec{k}} + a_{\vec{k}} a_{\vec{k}}^{\dagger}] ; \quad (36)$$

before normal ordering. For $a^{\dagger}; a$, the normal ordering prescription is

$$:a_{\vec{k}} a_{\vec{k}}^{\dagger} := a_{\vec{k}}^{\dagger} a_{\vec{k}} ; \quad (37)$$

since we imposed the usual canonical commutation relations. Hence the normal ordered Hamiltonian is

$$H = \sum_k a_k^y a_k^x + \frac{1}{2} \sum_k a_k^x a_k^y + \sum_k a_k^y a_k^y + \frac{1}{2} \sum_k a_k^x a_k^x H^+ H^- : \quad (38)$$

However, the reason why this is not a good Hamiltonian on the orbifold is that it generates time translations in t . It is associated with a preferred time direction on the covering space, as it is the energy operator associated with the Killing vector ∂_t . The individual pieces H generate time translations in t directions. The orbifold identifies the two, hence on the covering space neither direction is preferred. So the theory on the covering space must start with a symmetric combination of the two Hamiltonians H . Indeed, the energy operator (33) which we defined above is

$$H_{\text{inv}} = \frac{H^+ + H^-}{2} : \quad (39)$$

with zero point energies included. Note that the Z_2 invariance also extends to the zero energy contributions. We can then evaluate the vacuum energy on the orbifold,

$$\begin{aligned} h_0 \mathcal{H}_{\text{inv}} \mathcal{D}_{\text{inv}} &= \frac{1}{2} h_0 H^+ \mathcal{D}_i + \frac{1}{2} h_0 H^- \mathcal{D}_i \\ &= \frac{1}{2} h_0 \sum_k \frac{1}{2} a_k^x a_k^y \mathcal{D}_i + \frac{1}{2} h_0 \sum_k \frac{1}{2} a_k^y a_k^x \mathcal{D}_i = \frac{1}{2} \sum_k a_k^x a_k^y : \end{aligned} \quad (40)$$

This is the usual vacuum divergence. The above calculation should be contrasted with the naive calculation

$$h_0 H \mathcal{D}_i = h_0 (H^+ - H^-) \mathcal{D}_i = \frac{1}{2} \sum_k a_k^x a_k^y - \frac{1}{2} \sum_k a_k^y a_k^x = 0 ; \quad (41)$$

which is not Z_2 symmetric. Note also that the invariant Hamiltonian H_{inv} is bounded from below, since the notion of "boundedness" depends on the direction of time and both directions are identified.

The invariant Hamiltonian operator (39) must derive from an invariant stress tensor. Thinking of the latter as an operator, it will also reduce to components which act on the subspaces H . In our notation, the invariant stress tensor should be written

$$T^{\text{inv}}(t; x) = \frac{T^+(t; x)}{T^-(t; x)} = \frac{\mathcal{C}_+ + \mathcal{C}_-}{\mathcal{C}_+ - \mathcal{C}_-} : \quad (42)$$

We can now present an improved (completely Z_2 invariant) version of the calculation of the vacuum expectation value of the stress tensor. Recall that the initial condition creates

subtleties near $t = 0$, so we first assume $\mathbf{j}j > 0$ so that we can trust the mode expansions. Then, simply

$$\begin{aligned}
 \text{inv} h_0 T^{\text{inv}}(\mathbf{x}) \mathbf{j}i_{\text{inv}} &= \frac{1}{2} h_0 \mathbf{j}h_0 \frac{T^+(\mathbf{x})}{T^-(\mathbf{x})} \frac{\mathbf{j}i}{\mathbf{j}i} \\
 &= \lim_{\mathbf{x}^0 \rightarrow 0} \frac{1}{2} h_0 \mathbf{j} + (\mathbf{x})^0 + (\mathbf{x}^0) \mathbf{j}i + h_0 \mathbf{j} - (\mathbf{x})^0 - (\mathbf{x}^0) \mathbf{j}i \\
 &= \lim_{\mathbf{x}^0 \rightarrow 0} \frac{1}{2} \frac{1}{(\mathbf{x} - \mathbf{x}^0)^2} + \frac{1}{(\mathbf{x} - \mathbf{x}^0)^2} = \lim_{\mathbf{x}^0 \rightarrow 0} \frac{1}{(\mathbf{x} - \mathbf{x}^0)^2} : \quad (43)
 \end{aligned}$$

This is again just the usual vacuum divergence. The renormalized expectation value of T_{inv} would then be equal to zero. There are two main differences with the previous calculation of Section 2: i) Everything is Z_2 invariant, including the vacuum state. ii) Essentially, (\mathbf{u}) is now replaced by \mathbf{j} . But \mathbf{j} are decoupled, so there are no " $h_0 \mathbf{j} + \mathbf{j}i$ " cross contractions, as were depicted in Fig. 5. Near the initial slice $t = 0$ the situation is more subtle. As noted previously, the antisymmetric part of the fields must die off sufficiently rapidly. Such behavior will alter the mode expansion of the fields. If we insist on trusting the mode expansion everywhere at $t \neq 0$, then we must switch off the antisymmetric parts abruptly with step functions:

$$+ \mathbf{j}_A(t; \mathbf{x}) = (1 - \delta(t)) \mathbf{j}(\mathbf{x}); \quad \mathbf{j}_A(-t; \mathbf{x}) = (1 - \delta(-t)) \mathbf{j}(\mathbf{x}); \quad (44)$$

separating out the time dependence. But then the tt component of the invariant stress tensor will have a $\delta^2(t)$ singularity and the $t\mathbf{x}^i$ components a $\delta(t)$ singularity at the initial slice $t = 0$. However, if we interpret the R^{1+1}/Z_2 orbifold as a toy model of cosmology, then $t = 0$ slice plays the role of the initial singularity. Having a divergent stress tensor at the $t = 0$ slice is then natural in such a cosmological interpretation | it could represent the necessity for appropriate boundary conditions.

Moreover, we are really interested in strings on R^{1+1}/Z_2 , and one should recall that there is a twisted sector which is localized at the singularity. The initial divergence of the stress tensor is related to the intricate story of whether the orbifold singularity can be blown up and whether the singular geometry really is the actual geometry on which to consider the QFT.

The main point that we would like to stress here is that the stress tensor does not diverge in the boundary of the CTC region. That kind of a singularity would have been a signal of a more serious instability. The reason why it does not happen, without conflict of the chronology protection conjecture, is that in the reformulation of QFT it is apparent that nothing actually propagates along a CTC. Instead of a single quantum propagating around and around in a CTC, there is a quantum and its copy which propagate in opposite directions.

Sum m ary. We have presented a Z_2 formulation of QFT, needed as a starting point to define QFT on the R^{1+1}/Z_2 orbifold. In particular, we presented a new, invariant derivation of the vacuum expectation value hT in. It turns out to have the same form as if there was no orbifold, except at the initial slice $t = 0$ which can be interpreted as the "big bang", thinking of the orbifold as a toy cosmological model. This initial divergence is the only pathology from the time-nonorientability of the orbifold. Everywhere away from the $t = 0$ slice the local physics is well defined.

In the following sections, we will calculate the backreaction in string theory, using standard orbifold techniques. The result turns out to be the same: the vev has the same form as if the target space were Minkowski space instead of the orbifold. If one were to have performed the string calculation first (as we in fact did), the result would seem puzzling. However, in the light of the invariant formulation of QFT on the orbifold, it appears natural. Further, at low energies string theory should reduce to QFT: since the form must respect the symmetries of the orbifold, so must the latter. The low energy limit of string theory on R^{1+1}/Z_2 must be a symmetric QFT; the latter is precisely what we have formulated in this section.

We will now give some details of the complementary string theory calculation, and later return to a discussion of other aspects of the theory.

5 The Stress Tensor and the Graviton Tadpole

Our next goal is to calculate the backreaction on the orbifold at one-loop level in string theory. In practice, this is done by calculating the one-loop graviton tadpole.

If we write the metric tensor as $g(x) = \eta + 2h(x)$, the vev of the stress tensor may be written [50]

$$hT = \frac{i}{g} \ln Z_{\text{EFT}}^{\text{2nd}}|_{h=0} = \frac{i}{2} \frac{Z_{\text{1st}}}{h}|_{h=0} : \quad (45)$$

In the above, we used the relation between the vacuum amplitudes in the second quantized and first quantized formalism, $Z_{\text{2nd}} = e^{Z_{\text{1st}}}$, to replace the effective field theory action $\ln Z_{\text{EFT}}^{\text{2nd}}$ by the point particle partition function Z_{1st} .

Now we replace point particles by strings. At one-loop level [51]

$$Z_{\text{1 loop}}^{\text{ST}}[g] = \frac{d}{4} \frac{d}{2} Z(\) = \frac{d}{4} \frac{d}{2} \int \frac{Z}{T^2} D X e^{i \frac{T}{2} \int d^2 w g(x) \partial x \partial x} : \quad (46)$$

This is then inserted⁷ in (45). Suppressing the integral over T , we have

$$Z_{\text{1 loop}}^{\text{ST}} = \int D X e^{i \frac{T}{2} \int d^2 w \partial x \partial x} \left[1 + i \frac{g_{\text{str}}}{0} \int d^2 w h(x) \partial x \partial x \right] + : \quad (47)$$

⁷This is somewhat reminiscent of a recent calculation in [52].

Now Fourier expand the perturbation,

$$h(X) = \frac{d^{D+1}k}{(2)^{D+1}} e^{-ik \cdot X} (k) e^{ik \cdot X} \quad (48)$$

and introduce

$$V(k) = \partial X \partial X e^{ik \cdot X}; \quad (49)$$

then

$$Z_{1\text{ loop}}^{\text{ST}}[g] = Z_{1\text{ loop}}^{\text{ST}}[] + \frac{g_{\text{str}}}{4} \int_0^Z \frac{d^{D+1}k}{(2)^{D+1}} d^2 w e^{-ik \cdot w} (k) h V(k; w) i + \dots \quad (50)$$

We then get

$$h T(x)i = \frac{1}{4} \int_0^Z \frac{d^{D+1}k}{(2)^{D+1}} d^2 w h V(k; w) i e^{-ik \cdot x} \quad (51)$$

the relation between the Fourier transform ed tadpole and the stress tensor.

Note that in Minkowski space, one obtains

$$h V(k)i = \frac{g_{\text{str}}}{4} \frac{\frac{D+1}{2} \binom{D+1}{2} \delta_{0k}}{V_{D+1}} Z_{1\text{ loop}}; \quad (52)$$

so that

$$h T(x)i = \frac{1}{4^{13} V_{26}} Z_{1\text{ loop}} \quad (53)$$

which is of the right form for the stress tensor of a cosmological constant $Z_{1\text{ loop}}$.

On Z_2 orbifolds, the story is essentially the same. What is different in the string graviton tadpole calculation is that the relevant vertex operator must be Z_2 invariant: it is the sum of vertex operators carrying k and $-k$ in the directions of the orbifold. The Fourier transform of the tadpole will then be the sum

$$h T(X)i + h T(-X)i; \quad (54)$$

where X are the coordinates along the orbifold directions. This is obtained from the effective action by including the functional differentiation $= h(-X)$. By comparing with the discussion in Section 3, it can be seen that (54) corresponds to what we called

$$h T^+ i + h T^- i; \quad (55)$$

5.1 One-loop Graviton Tadpole

Now we proceed to give some of the details of the calculation of the one-loop graviton tadpole in string theory described above. Our calculations are based on the functional method. We begin with a brief review of the latter, following [51]. As it turns out, an immediate difference with tadpole calculations on Euclidean orbifolds is in kinematics and in appropriate choice of polarization of vertex operators. We have also performed the same calculations in the oscillator formalism. It also turns out that there are some interesting subtleties and differences with the standard discussion; detailed notes may be found in the appendix.

We should note that in the string computations, one usually performs a Wick rotation in both spacetime and worldsheet, necessary for formal convergence. If the target space is time-dependent, the standard techniques of analytic continuation may not be applicable.⁸ In the context of the $R^{1,3}/Z_2$ orbifold, the issue was already noted in [10]. In the present paper, we simply adopt the same strategy as in [10], namely we formally continue to Euclidean signature in the calculations to obtain an expression for the tadpole, which we then formally continue back to Lorentzian signature. The result turns out to be well defined and compatible with the low-energy limit, the invariant field theory calculation of Section 4. In that section, propagation on the orbifold was essentially shown to be an identification of forward and backward propagation on the covering space $R^{1,3}$. This may also explain why the formal analytic continuation prescription continues to work in the calculations of this section.

5.2 The generating functional on $R^{1,3}$

Following [51], the generating functional is

$$Z[J] = \text{exp} \int d^2w J(w;w) X(w;w) : \quad (56)$$

In order to perform the functional integrals, we introduce a complete set eigenmodes X_I of the Laplacian r^2 on the toroidal worldsheet,

$$\begin{aligned} \int r^2 X_I(w;w) &= \delta_I^2 X_I(w;w) ; \\ d^2w X_I(w;w) X_J(w;w) &= \delta_{IJ} \end{aligned} \quad (57)$$

and expand the string embedding coordinates in the eigenmodes,

$$X(w;w) = \sum_I \frac{p}{4} \delta^{2,0} X_I X_I(w;w) : \quad (58)$$

⁸See e.g. [53] for a proposal to modify the standard approach.

We also denote

$$J_{,I} = \frac{p}{4^{2^0}} \int d^2w J(w;w) X_I(w;w) : \quad (59)$$

We then integrate out the expansion coefficients x_I by completing the squares in the generating functional and performing the resulting Gaussian integrals. In particular, the integrals will include zero mode contributions from x_0 . The result in d target space dimensions is

$$Z[J] = N[J_0] \det^0 r_w^2 \int d^2w \int_0^Z d^2w^0 J(w) G(w;w^0) J(w^0) ; \quad (60)$$

where $N[J_0]$ is the zero mode contribution

$$N[J_0] = i(2)^d \det^{(d)}(J_0) ; \quad (61)$$

(with i coming from the Wick rotation $x_I^0 \rightarrow ix_I^d$), the determinant factor is

$$\det^0 r_w^2 \prod_{I \neq 0}^Y \frac{1}{!_I^2} ; \quad (62)$$

and $G^0(w;w^0)$ is the Green's function

$$G^0(w;w^0) = \prod_{I \neq 0}^X \frac{2}{!_I^2} X_I(w) X_I(w^0) : \quad (63)$$

The latter satisfies the differential equation

$$\frac{1}{2} r_w^2 G^0(w;w^0) = g^{1=2} (w - w^0) X_0^2 ; \quad (64)$$

where X_0 is the zero mode of the Laplacian on the torus. The functional determinant (62) gives the torus partition function,

$$Z_{T^2}[0] = V_d \det^0 r_w^2 \quad (65)$$

5.3 The generating functional on Orbifolds

Next we generalize this to the case of the orbifold. For comparison, we will consider two related types of orbifolds:

A) The Euclidean orbifold $R^{1,d} / R^{25-d} = Z_2$

B) The Lorentzian orbifold $R^{1,d} / Z_2 \times R^{25-d}$.

We split the coordinates X and the components of the source J into those parallel (k) and transverse (l) to the orbifold directions. The generating functional takes the form

$$Z[J] = \sum_{g=0}^{X^1 X^2} \sum_{h=0}^{Z} \text{expf} \int d^2w \sum_{k} J_k X^k + i \sum_{l} J_l X^l g_{gh} \quad (66)$$

including the sum over the untwisted ($g = 1$) and twisted ($g = 0$) sectors, with ($h = 0$) and without ($h = 1$) the Z_2 reaction, for string oscillations in the orbifolded directions. We then again expand X in the eigenmodes of r^2 , but now the eigenvalues and modes will be different in the orbifolded directions for each sector, due to the different (anti)periodic boundary conditions. After integrating over the eigenmode coefficients, the functional takes the form

$$Z[J] = \frac{N_{(1)}[J_0]}{N_{(0)}[0]} Z_{(0)} \expf \frac{1}{2} \int d^2w \sum_{k} d^2w^0 J_k(w) \sum_l J_l(w^0) G^0(w; w^0) g + \sum_{gh} \frac{N_{(g,h)}[J_0]}{N_{(g,h)}[0]} Z_{(g,h)} \expf \frac{1}{2} \int d^2w \sum_{k} d^2w^0 J_k(w) \sum_l J_l(w^0) G^0_{(g,h)}(w; w^0) g: \quad (67)$$

In the above, $N_{(1)}[J_0]$, $N_{(0)}[J_0]$ are the zero mode contributions. In the orbifolded directions, there are zero modes only in the untwisted sector without the Z_2 reaction, and none in the other sectors because X satisfies an antiperiodic boundary condition in at least one of the toroidal worldsheet directions. Thus, for $J = k^{(2)}(w - w^0)$,

$$\frac{N_{k;(1;1)}[J_0]}{N_{k;(1;1)}[0]} = \frac{1}{V_{d+1}} \quad (d+1) \quad (k); \quad N_{k;(g,h)}[k] = 1 \text{ for } (g,h) \notin (1;1) : \quad (68)$$

The factors $Z_{(0)}$, $Z_{(g,h)}$ are the partition function contributions from the directions transverse to and parallel with the orbifold, including the four untwisted and twisted (g,h) -sectors. Explicitly [10],

$$Z_{k;(1;1)} = \frac{V_{25-d}}{2} \frac{1}{P \frac{1}{2}^{25-d}} \quad (69)$$

$$Z_{k;(g,h)} = \frac{1}{g h} \quad (g,h) \notin (1;1)$$

There are four different Green's functions, corresponding to the different periodicities on the toroidal worldsheet. The doubly periodic one is [51]

$$G^0_{(1;1)}(w; w^0) \quad G^0(w; w^0) = -\frac{1}{2} \ln \int_{11}^0 \frac{w - w^0}{2}^2 + \alpha X_0^2 [\text{Im}(w - w^0)]^2; \quad (70)$$

and the other ones with at least one antiperiodic direction are

$$\begin{aligned}
 G_{(1;0)}^0(w;w^0) &= \frac{1}{2} \ln \frac{\overset{0}{\underset{11}{\ln}} \left(\frac{w-w^0}{4} j \right) \overset{10}{\underset{00}{\ln}} \left(\frac{w-w^0}{4} j \right)^2}{\overset{0}{\underset{00}{\ln}} \left(\frac{w-w^0}{4} j \right) \overset{01}{\underset{10}{\ln}} \left(\frac{w-w^0}{4} j \right)} \\
 G_{(0;1)}^0(w;w^0) &= \frac{1}{2} \ln \frac{\overset{0}{\underset{11}{\ln}} \left(\frac{w-w^0}{4} j \right) \overset{01}{\underset{10}{\ln}} \left(\frac{w-w^0}{4} j \right)^2}{\overset{0}{\underset{10}{\ln}} \left(\frac{w-w^0}{4} j \right) \overset{00}{\underset{00}{\ln}} \left(\frac{w-w^0}{4} j \right)} \\
 G_{(0;0)}^0(w;w^0) &= \frac{1}{2} \ln \frac{\overset{0}{\underset{11}{\ln}} \left(\frac{w-w^0}{4} j \right) \overset{00}{\underset{01}{\ln}} \left(\frac{w-w^0}{4} j \right)^2}{\overset{0}{\underset{01}{\ln}} \left(\frac{w-w^0}{4} j \right) \overset{00}{\underset{10}{\ln}} \left(\frac{w-w^0}{4} j \right)} : \quad (71)
 \end{aligned}$$

In n -point amplitudes, one also encounters self-contractions which require renormalization. A simple prescription is to subtract the divergent part $\frac{1}{2} \ln j w^0 j$ from the Green's functions and define their renormalized versions. The renormalized version of G_{11}^0 is [51]

$$G_{(1;1);ren}^0(w;w) = \frac{1}{2} \ln \frac{\overset{0}{\underset{1}{\ln}} (0j)^2}{2} : \quad (72)$$

After some manipulations, the renormalized versions of the other Green functions also turn out to simplify considerably to the following simple forms:

$$G_{(g;h);ren}^0 = \frac{1}{2} \ln j_{gh} (0j)^4 : \quad (73)$$

for $(g;h) \in (1;1)$.

5.4 One-loop graviton tadpole on the orbifold

Consider then the one-loop graviton tadpole on the orbifold. The vertex operator for a state which is not projected out by the Z_2 reflection must be symmetric under $X \leftrightarrow -X$, hence the relevant massless tadpole on the orbifold is

$$\begin{aligned}
 hV(k_k; k_?) + V(-k_k; k_?)i \\
 = \frac{2g_{str}}{0} h @ X @ X e^{ik_k X_{jj} + ik_? X_?} + @ X @ X e^{-ik_k X_{jj} + ik_? X_?} i \quad (74)
 \end{aligned}$$

The momentum must satisfy the on-shell condition $k^2 = m^2 = 0$. Now there are some immediate choices to be done where the Euclidean and Lorentzian orbifolds A and B differ. In string theory one often considers Euclidean orbifolds as a way of compactifying extra dimensions. Therefore one is usually interested in states which only propagate and carry polarization in the non-orbifolded noncompact directions, and the momentum and the polarization are chosen to be entirely transverse to the orbifold, with $k^2 = k_?^2 = m^2$.

However, in the Lorentzian orbifold one must also include components in parallel directions in order to satisfy the on-shell condition. Further, let us make the usual simplifying choice for the polarization and assume it to be polarized only in the first $d+1$ spacetime directions. That is, the $\partial X \partial X$ part of the vertex operator will contribute only when $\vec{k} = 0$. Note that the polarization part is then invariant under $X \rightarrow X + \vec{k}$. Then also the polarization is parallel to the orbifolded directions.

Let us illustrate this by calculating the tadpole in both cases A and B, with the kinematics

A) (Euclidean case) $k = (k_\mu; k_\nu) = (k_\mu; 0)$ with $k_\mu^2 = 0$

B) (Lorentzian case) $k = (k_\mu; k_\nu)$ with $k^2 = k_\mu^2 + k_\nu^2 = 0$.

We evaluate the tadpole by first performing a point splitting and then functional differentiation of the generating functional,

$$h \partial X(w; w) \partial X(w; w) e^{ikX(w; w)} i = \frac{1}{Z} \left(-i \lim_{w_1, w_2 \rightarrow w} \frac{\partial_{w_1} \partial_{w_2}}{J(w_1)} \frac{\partial_{w_1} \partial_{w_2}}{J(w_2)} \exp \frac{d^2 w^0 J(w^0) X(w^0) g i}{2} \right) \quad (75)$$

evaluated at $J(w^0) = k^{(2)}(w^0 - w)$. Before the functional differentiation, for the generating functional we substitute the integrated form (67). We will also substitute the on-shell condition $k^2 = 0$.

In the Euclidean case, the functional differentiation and the on-shell condition leaves

$$h \partial X(w) \partial X(w) e^{ikX} i = \frac{N_2[k]}{N_2[0]} Z_k \left[\frac{1}{Z_k(g; h)} \right] \lim_{w_1, w_2 \rightarrow w} \left[\partial_{w_1} \partial_{w_2} G^0(w_1; w_2) - k \cdot k \partial_{w_1} G^0(w_1; w) \partial_{w_2} G^0(w_1; w) \right] \frac{1}{Z_k(g; h)} \quad (76)$$

whereas in the Lorentzian case, the corresponding result is

$$h \partial X(w) \partial X(w) e^{ikX} i = \frac{N_2[k]}{N_2[0]} Z_k \left[\frac{1}{Z_k(g; h)} \right] \lim_{w_1, w_2 \rightarrow w} \left[\partial_{w_1} \partial_{w_2} G^0_{(g; h)}(w_1; w_2) - k \cdot k \partial_{w_1} G^0_{(g; h)}(w_1; w) \partial_{w_2} G^0_{(g; h)}(w_1; w) \right] \frac{1}{Z_k(g; h)} \quad (77)$$

In both cases, the Green's function will need to be replaced by their renormalized versions. We can already see that the expressions are quite different. Let us simplify them further.

First, we can use the equation (64) to simplify the double derivatives of the Green's functions. First, since $G^0(w_1; w_2) = G^0(w_1 - w_2)$,

$$\partial_{w_1} \partial_{w_2} G^0(w_1; w_2) = \partial_{w_1} \partial_{w_1} G^0(w_1; w_2) : \quad (78)$$

On the other hand, the equation (64) evaluates to

$$\partial_w \partial_w G^0(w; w^0) = -\frac{1}{2} (w - w^0)^2 + \frac{0}{2} X_0^2 : \quad (79)$$

The first term on the right hand side originates from the short distance divergence $G^0(w_1; w_2) \sim \ln |w_1 - w_2|^2$ of the Green's function, which we subtract off when we renormalize the Green's functions. The latter then satisfy the equation

$$\partial_{w_1} \partial_{w_2} G_{\text{ren}}^0(w_1; w_2) = -\frac{0}{2} X_0^2 : \quad (80)$$

Similar results hold for the renormalized Green's functions $G_{(g,h); \text{ren}}^0$ in the Lorentzian orbifold case. Since a zero mode X_0 exists only in the doubly periodic $(g;h) = (1;1)$ sector, the double derivatives $\partial \partial G_{(g,h); \text{ren}}^0$ vanish in all the other three sectors.

Next, we examine the first derivatives of the renormalized Green's functions. A calculation shows that in all cases the Green's functions have a short distance behavior of the type

$$\partial G_{(g,h)}^0(w; w^0) \underset{w \rightarrow w^0}{=} -\frac{0}{2} (w - w^0)^{-1} + C_{(g,h)}(\) (w - w^0) + O((w - w^0)^3) \quad (81)$$

where $C_{(g,h)}(\)$ are rational functions of derivatives of theta functions at (0) . A similar formula is found for the antiholomorphic derivative $\partial G_{(g,h)}^0$. There is only one divergent term, due to the self-contraction of X with ∂X . The renormalization prescription again removes the divergent term, so the renormalized (derivatives of) Green's function vanish in the limit $w \rightarrow w^0$. Hence these terms will not contribute to the graviton tadpole.

Substituting all the normalization and partition function factors, the final results are

$$hV(k) + V(-k) \underset{\text{loop}}{=} \frac{g_{\text{str}}}{4} \frac{\underset{g,h}{(25)}(k)}{V_2} Z_2 \underset{g,h}{[\]} Z_{k,(g,h)}[\] : \quad (82)$$

for the graviton tadpole in the Euclidean orbifold, and

$$hV(k) + V(-k) \underset{\text{loop}}{=} \frac{g_{\text{str}}}{4} \frac{\underset{g,h}{(26)}(k)}{V_{26}} Z_2(-) Z_{k,(1;1)}[\] : \quad (83)$$

for the tadpole in the Lorentzian orbifold. At first, the final result looks rather surprising, as it is precisely the same as for a graviton in the usual $R^{1/25}$ target space! However, in

the light of the analysis of the Section 4, this is precisely what we expect. The low-energy limit of invariant field theory tells us that the vacuum expectation value of free field theory on the orbifold has the same form as in ordinary Minkowski space. The expectation value is just the vacuum zero-point energy of bosonic string theory. By analogy, one would then expect the tadpole to vanish for the superstring.

6 Time Evolution and Local Symmetries on the Fundamental Domain

In all previous discussions, we limited the analysis to what corresponds to free field theory in the low-energy limit. What then of the interacting theory? Given that the orbifold is globally time-nonorientable, is there any way of defining symmetries at least locally, for example away from the $t = 0$ axis in the above choice of the fundamental domain? Let us first illustrate the problem with a simple figure. Figure 8 depicts a point particle and

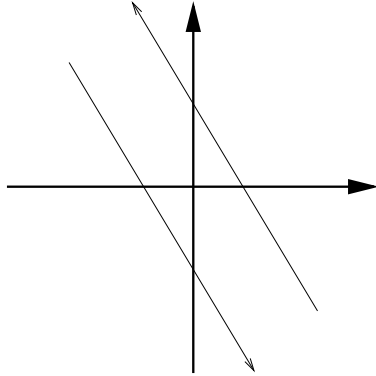


Figure 8: Example of a point particle and its image propagating on the covering space.

its image propagating in opposite time and space directions on the covering space. As discussed in Section 4, both trajectories will be identified by the \mathbb{Z}_2 reflection, resulting in a single trajectory for a point particle on the fundamental domain. The details depend on the choice of the fundamental domain.

Consider first choosing the right half-space as the fundamental domain, and drawing the corresponding "pocket", as depicted in Figure 9 (see also Figs. 2(a) and 3). Alternatively, we can choose the upper half-space as the fundamental domain, and identify the negative x -axis with the positive x -axis. The result is depicted in Figure 10 (see also Figs. 2(b) and 4).

As discussed in Section 2, a possible choice for the time-arrow on the fundamental domain of Figure 9 is to let it point from the lower right quadrant to the upper right

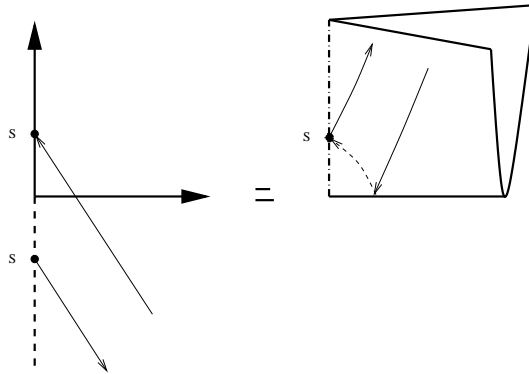


Figure 9: Point particle propagating on the fundamental domain ain . The left part of the figure depicts the fundamental domain ain , with the dashed negative time axis ($x = 0$) identified with the positive time axis. For example, the points S marked with a black dot are identified. The identification results in the pocket shown on the right. The time orientation breaks down on the time axis. The part of the trajectory drawn with solid lines depicts propagation on the front fold of the pocket, while the dashed line depicts propagation on the rear fold. The point S is on dotted-dashed line, where the time direction becomes ill-defined.

quadrant, while becoming ambiguous on the $x = 0$ axis. On the pocket, time would thus flow down the front fold and continue upwards on the rear fold. Similarly, on the fundamental domain ain of Figure 10 one can choose the arrow of time to point upwards on the upper half-space, with the $t = 0$ axis as the origin of time. On the pocket, time would then flow upwards on both sides of the fold. However, then the trajectories depicted on the figures would seem to violate causality. On Figure 9, if we choose a constant time slice far up on the front fold, the trajectory will cross it twice. First it crosses the slice on its way down along the front fold, then it continues to the other side but returns back to the front slice and crosses the slice again. On Figure 10, the trajectory would propagate first backwards in time towards $t = 0$, then propagate forward in time on the rear fold and again on the front fold. Both interpretations are troublesome.

However, we can improve the situation a bit. In Section 4, we identified forward time evolution of a particle with backward time evolution of its image on the covering space. We start the forward evolution from $t = -1$ and the backward evolution from $t = 1$. The time evolution continues without problems until we reach the dividing line between the two half-spaces, depending on the choice of the fundamental domain ain . That is, if we choose the right half-space as the fundamental domain ain , we can follow the time evolution until the particle and its image reach $x = 0$. If we choose the upper half-space as the fundamental domain ain , the time evolution can be followed up to $t = 0$. Similarly, just after

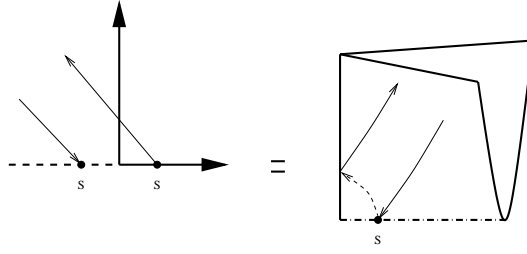


Figure 10: Point particle propagating on the fundamental domain. On the left figure, the points marked with S are identified. On the right figure, the solid lines depict propagation on the front fold of the pocket, the dashed line depicts propagation on the rear fold. The point marked with S is on the dotted-dashed line, where the time direction becomes ill-defined.

crossing the dividing line, we can again follow the time evolution onwards. For example, in the latter case we can continue from $t = 0 +$ the forward time evolution to $t = 1$ and backward evolution to $t = -1$. The problem is if and how it is possible to continue the evolution across the dividing line.

If we choose the upper half-space as the fundamental domain, it is simple to give a more formal definition. In the Heisenberg picture we define the invariant time evolution operator from t_0 to $t_1 > t_0$ on the covering space to be

$$\begin{aligned}
 U_{\text{inv}}(t_0; t_1) &= T \exp \left[i \int_{t_0}^{t_1} dt H_{\text{inv}}(t) \right] \\
 &= T \exp \left[\int_{t_0}^{t_1} dt H^+ \right] \Big|_0^0 \quad ! \\
 &= U^+(t_0; t_1) \Big|_0^0; \quad (84)
 \end{aligned}$$

where T denotes anti-time ordering. This is unambiguously defined if both $t_0, t_1 < 0$ or both $t_0, t_1 > 0$. Problems arise when $t_0 < 0$ and $t_1 > 0$.

Let us see what this means for the point particles in the figures. In Figure 8, we launch the particle and its image from $t = -1$ and $t = +1$, and then propagate them using $U(-1; t)$ towards the x-axis, i.e. up to $t = 0$. This gives the lower half and the upper half of the forward and backward trajectories of Fig. 8. They are identified on the fundamental domain, so this gives the 'downward' trajectory on the left part in Figure 10 all the way to the marked point S, and the downward trajectory to the point S on the front fold of the pocket in Figure 10. Similarly, we could propagate forward and backward from $t = 0 +$, giving the other halves of the trajectories in Figure 8. In Figure 10, the

resulting trajectory is the "upward" one on the left diagram, and the upward trajectory starting on the rear fold and continuing to the front fold of the pocket.

To summarize, on the fundamental domain (the pocket), we can either choose the time to point downwards, corresponding to Figure 2 b) with the arrows reversed, and consider time evolution up to a "big crunch" at $t = 0$, or choose the time to point upwards and consider time evolution forward from a "big bang". The latter corresponds to Figure 2 b). Either way, the evolution breaks down at $t = 0$. But that is also the point where from Section 4 we know the stress tensor to diverge⁹.

Consider then an interacting field theory. We could adopt the interaction picture, and define the time evolution operator as

$$U_{I,\text{inv}}(t_0; t_1) = \begin{pmatrix} R_{t_1} & 0 \\ T \exp [i \int_{t_0}^{R_{t_1}} dt d^d x L_I(+ (t; x))] g & T \exp [i \int_{t_0}^{R_{t_1}} dt^0 d^d x L_I(- (t^0; x))] g \end{pmatrix} ! \quad (85)$$

where L_I is the interaction part of the Lagrangian. We could consider this as the local S-matrix. Hence, as long as we stay away from the singular $t = 0$ hypersurface, the S-matrix has the same properties as that of an ordinary field theory on Minkowski space.

Acknowledgment

We would like to thank Vijay Balasubramanian, Fawad Hassan, and Asad Naqvi for the collaboration which lead us to this investigation, and many discussions on the interpretational issues. We also thank Per Kraus for helpful discussions and useful encouragement. EK-V was in part supported by the Academy of Finland, and thanks the University of California at Los Angeles and University of Pennsylvania for hospitality at different stages of this work. RGL was supported by US DOE under contract DE-FG 02-91ER 40677 and thanks the Helsinki Institute of Physics for hospitality. ES would like to thank A. Lawrence, S. Kachru, A. Knutson and R. Bryant for helpful conversations. EK-V would like to dedicate this work to Anne Keski-Vakkuri, who was conceived and born during this project.

Appendix

In this appendix, we will provide the details of complementary calculations using oscillator methods. There are several subtleties that are not regularly seen in the usual backgrounds.

⁹Similar analysis, based on the other two choices of the fundamental domain, Figure 2 a) and c), are also possible. Then the time evolution would break down at $x = 0$ (a) or at null cone (c).

We will use the notation where \tilde{k} is the image of k under the orbifold.

$$\tilde{k}_o = -k_o \quad (86)$$

$$\tilde{k}_u = +k_u \quad (87)$$

We want to evaluate

$$T(\) = \frac{1}{2} \text{tr}_{U+T} (1 + \hat{g}) \int d^2z V(z; z) q^{L_o} \bar{q}^{L_o} \quad (88)$$

It is important to note that in this formalism, obtained by sewing the cylinder into a torus, there are zero modes in the U sectors of the trace, but not in the twisted T sectors. The massless vertex operator is of the form

$$V(z; z) = \frac{2g_{\text{str}}}{0} : @X @X \frac{1}{2} e^{ik \cdot X(z; z)} + e^{i\bar{k} \cdot \bar{X}(z; z)} : \quad (89)$$

The non-zero mode portion of this expression can be evaluated using coherent state methods. For each oscillator j_n ($n > 0$) we introduce a coherent-state basis $|j_n\rangle$ and write the trace as a $\langle \rangle$ -integral. If the $\langle @X \rangle$ does not contribute an oscillator, we find (for each $n > 0$ and $\langle \rangle$)

$$\int^Z \frac{d^2}{\bar{z}} e^{\langle j \cdot \bar{z} \rangle} e^{0_{k^2=4n}} \langle \frac{p}{j} \frac{0_{=2k}}{z^n} e^{\frac{p}{j} \frac{0_{=2k}}{z^n}} \rangle \quad (90)$$

for the 1-insertion, while for the \hat{g} -insertion, we get

$$\int^Z \frac{d^2}{\bar{z}} e^{\langle j \cdot \bar{z} \rangle} e^{0_{k^2=4n}} \langle \frac{p}{j} \frac{0_{=2k}}{z^n} e^{\frac{p}{j} \frac{0_{=2k}}{z^n}} \rangle \quad (91)$$

This is a standard integral whose evaluation can be found in [54]. The result is

$$\frac{1}{1 - \frac{q^n}{q}} e^{-0_{k \cdot k} \frac{q^n}{2n(1 - q^n)}} \quad (92)$$

again for each $n > 0$ and $\langle \rangle$. For the \sim oscillators, we will get the same result, with q replaced by q . Now by simple re-ordering of sums and appropriate¹⁰ renormalization, we may compute:

$$\sum_{n \geq 2} \frac{1}{z^n} \frac{q^n}{1 + q^n} = \frac{2(\)}{q^{1-8}}; \quad \sum_{n \geq 2} \frac{1}{z^n} \frac{q^n}{1 + q^n} = \langle_{3,4} (\) \quad (93)$$

¹⁰In particular, there is a factor of 2 which must be absorbed by the (implicit) regulator in the first equation. This can be seen, for example, as a requirement of modular invariance.

On the other hand, the ∂X might contribute an oscillator. Then, we have a new matrix element

$$X \stackrel{Z}{\overbrace{\frac{d^2}{\partial^2}}} e^{j\frac{p}{2k}} \left(\frac{p}{2k} e^{j\frac{p}{2k}} z^{n-m} z^{m-1} + z^{m-1} z^{n-m} e^{j\frac{p}{2k}} z^{n-m} \right) \quad (94)$$

$m > 0$

When $m = n$, we find, recalling that $[m; e^a] = m a e^{a-m}$ and $j_n = e^{-n} \frac{p}{2k} j_0$

$$\frac{p}{2k} \frac{Z}{z} \frac{d^2}{\partial^2} e^{j\frac{p}{2k}} z^{m-n} q^m + z^n \left(j_0 e^{j\frac{p}{2k}} z^{n-m} e^{j\frac{p}{2k}} z^{n-m} j_0 \right) \quad (95)$$

$$= \frac{p}{2k} \frac{Z}{z} \frac{d^2}{\partial^2} e^{(1-q^m)j\frac{p}{2k}} z^{m-n} q^m + z^n e^{k(z^m - z^{m-n} q^m)} = \frac{p}{2k} \quad (96)$$

It is straightforward to show that this vanishes. Thus only the zero mode part of the ∂X factors contribute. As a corollary then, only the untwisted sector will contribute to the massless tadpole in the Lorentzian orbifold.

It remains to evaluate the zero modes. These are

$$\begin{aligned} U;1 : & \frac{Y}{2} \frac{dp}{2} \frac{p}{2} \frac{p}{2} e^{j\frac{p}{2k}} e^{(0-2)k\frac{p}{2} \ln j_0} j_0 + k_0 j_0 = \frac{Y}{2} \frac{p}{2} \frac{p}{2} \frac{p}{2} \\ U;\hat{g} : & \frac{Y}{2} \frac{dp}{2} \frac{p}{2} \frac{p}{2} e^{j\frac{p}{2k}} e^{(0-2)k\frac{p}{2} \ln j_0} j_0 + k_0 j_0 = \\ & = \frac{Y}{2} \frac{e^{2k_0^2=4}}{2} \frac{k_0 k_0=4}{2} ; \frac{2}{2} = \frac{2}{2} \end{aligned} \quad (97)$$

each times a factor $\frac{Q}{2} \frac{1}{j_0} \frac{Q}{u} \frac{p}{2}$. In the first case, this is multiplied by $X_{1,1} = j_0 j^{24}$, while in the second, we have $X_{1,0} = \frac{Q}{u} j_0^{-1} (1 - q^u)^{d-23} (1 + q^u)^{-(d+1)} j_0$. Thus, if we go on-shell, we get

$$T_0 = \frac{g_{str}}{2} \frac{Y}{u} \frac{p}{2} \frac{p}{2} \frac{p}{2} \frac{Y}{2} \frac{p}{2} \frac{p}{2} X_{1,1} + 2 \frac{Y}{2} \frac{p}{2} \frac{p}{2} X_{1,0} \quad ! \quad (98)$$

if ; are in the unorbifolded directions, while if they are in the orbifolded directions

$$T_0 = \frac{g_{str}}{2} \frac{Y}{u} \frac{p}{2} \frac{p}{2} \frac{p}{2} \frac{Y}{2} \frac{p}{2} \frac{p}{2} X_{1,1} + \frac{k_0 k_0}{4} 2 \frac{Y}{2} \frac{p}{2} \frac{p}{2} X_{1,0} \quad ! \quad (99)$$

This result is not modular invariant. However there is an ordering ambiguity¹¹ in zero modes from the $(U;\hat{g})$ sector that we have not taken into account. To see the problem, suppose we write the vertex operator as

$$V = \partial X \partial X e^{ikX} + \partial X e^{ikX} \partial X + e^{ikX} \partial X \partial X \quad (100)$$

¹¹ This ambiguity does not appear for Euclidean orbifolds.

Then, the $k \cdot k = 4$ in eq. (99) is multiplied by $+ 2 + \dots$. There is a modular invariant choice ($+ + = 1, - = -1$) for which the kk term cancels. (There is no effect of this ordering issue.) We then obtain (In the notation of Section 5, $X_{1;1} = \frac{1}{\sqrt{26}} Z_{k;(1;1)} Z_{?}$)

$$T_0 = \frac{g_{\text{str}}}{4} \frac{(26)(k)}{V_{26}} Z_{k;(1;1)} [] Z_{?} [] \quad (101)$$

(for $;$ in the orbifold directions). This result agrees with the result in Section 5 for the case of the Lorentzian orbifold.

References

- [1] G. T. Horowitz and A. R. Steif, "Singular string solutions with nonsingular initial data," *Phys. Lett. B* 258 (1991) 91{96.
- [2] C. R. Nappi and E. Witten, "A closed, expanding universe in string theory," *Phys. Lett. B* 293 (1992) 309{314, [hep-th/9206078](#).
- [3] C. Kounnas and D. Lust, "Cosmological string backgrounds from gauged WZW models," *Phys. Lett. B* 289 (1992) 56{60, [hep-th/9205046](#).
- [4] E. Kiritsis, "Duality symmetries and topology change in string theory," [hep-th/9309064](#).
- [5] E. J. Martinec, "Space-like singularities and string theory," *Class. Quant. Grav.* 12 (1995) 941{950, [hep-th/9412074](#).
- [6] A. E. Lawrence and E. J. Martinec, "String field theory in curved spacetime and the resolution of spacelike singularities," *Class. Quant. Grav.* 13 (1996) 63{96, [hep-th/9509149](#).
- [7] J. Khoury, B. A. Ovrut, N. Seiberg, P. J. Steinhardt, and N. Turok, "From big crunch to big bang," *Phys. Rev. D* 65 (2002) 086007, [hep-th/0108187](#).
- [8] N. Seiberg, "From big crunch to big bang - is it possible?", [hep-th/0201039](#).
- [9] G. Veneziano, "String cosmology: The pre-big bang scenario," [hep-th/0002094](#).
- [10] V. Balasubramanian, S. F. Hassan, E. Keski-Vakkuri, and A. Naqvi, "A spacetime orbifold: A toy model for a cosmological singularity," *Phys. Rev. D* 67 (2003) 026003, [hep-th/0202187](#).

- [11] N .A .Nekrasov, *\M ike universe, tachyons, and quantum group,"* hep-th/0203112.
- [12] L.Cornalba and M .S.Costa, *\A New Cosmological Scenario in String Theory,"* Phys. Rev. D 66 (2002) 066001, hep-th/0203031.
- [13] J.Simon, *\The geometry of null rotation identifications,"* JHEP 06 (2002) 001, hep-th/0203201.
- [14] H .Liu, G .M oore, and N .Seiberg, *\Strings in a time-dependent orbifold,"* JHEP 06 (2002) 045, hep-th/0204168.
- [15] H .Liu, G .M oore, and N .Seiberg, *\Strings in time-dependent orbifolds,"* JHEP 10 (2002) 031, hep-th/0206182.
- [16] G .T .Horowitz and J.Polchinski, *\Instability of spacelike and null orbifold singularities,"* Phys. Rev. D 66 (2002) 103512, hep-th/0206228.
- [17] A .Lawrence, *\On the instability of 3D null singularities,"* JHEP 11 (2002) 019, hep-th/0205288.
- [18] M .Fabinger and J.M oore, *\On smooth time-dependent orbifolds and null singularities,"* hep-th/0206196.
- [19] S.Elitzur, A .G iveon, D .Kutasov, and E .Rabinovici, *\From big bang to big crunch and beyond,"* JHEP 06 (2002) 017, hep-th/0204189.
- [20] B .Craps, D .Kutasov, and G .Rajesh, *\String propagation in the presence of cosmological singularities,"* JHEP 06 (2002) 053, hep-th/0205101.
- [21] J.Simon, *\Null orbifolds in AdS, time dependence and holography,"* JHEP 10 (2002) 036, hep-th/0208165.
- [22] O .Aharony, M .Fabinger, G .T .Horowitz, and E .Silverstein, *\Clean time-dependent string backgrounds from bubble baths,"* JHEP 07 (2002) 007, hep-th/0204158.
- [23] A .Buchel, P .Langfelder, and J.W alder, *\On time-dependent backgrounds in supergravity and string theory,"* Phys. Rev. D 67 (2003) 024011, hep-th/0207214.
- [24] M .A lishahiha and S .Parvizi, *\Branes in time-dependent backgrounds and AdS/CFT correspondence,"* JHEP 10 (2002) 047, hep-th/0208187.
- [25] E .D udas, J.M ourad, and C .T imirgaziu, *\Time and space dependent backgrounds from nonsupersymmetric strings,"* hep-th/0209176.

[26] M . Berkooz, B . Craps, D . Kutasov, and G . Rajesh, \Comments on cosmological singularities in string theory," hep-th/0212215.

[27] A . J. Tolley and N . Turok, \Quantum fields in a big crunch / big bang spacetime," Phys. Rev. D 66 (2002) 106005, hep-th/0204091.

[28] C . Gordon and N . Turok, \Cosmological perturbations through a general relativistic bounce," hep-th/0206138.

[29] J. Figueroa-O'Farrill and J. Simón, \Supersymmetric Kaluza-Klein reductions of M 2 and M 5 branes," hep-th/0208107.

[30] M . Fabinger and S . Hellerman, \Stringy resolutions of null singularities," hep-th/0212223.

[31] A . Hashimoto and S . Sethi, \Holography and string dynamics in time-dependent backgrounds," Phys. Rev. Lett. 89 (2002) 261601, hep-th/0208126.

[32] L . Cornalba and M . S . Costa, \On the classical stability of orientifold cosmologies," hep-th/0302137.

[33] S . W . Hawking, \The Chronology protection conjecture," Phys. Rev. D 46 (1992) 603611.

[34] M . Visser, \The quantum physics of chronology protection," gr-qc/0204022.

[35] B . S . Kay, \The principle of locality and quantum field theory on (nonglobally hyperbolic) curved space-times," Rev. Math. Phys. 5 II (1992) 167.

[36] A . Chamblin and G . W . Gibbons, \A Judgment on spinors," Class. Quant. Grav. 12 (1995) 2243{2248, gr-qc/9504048.

[37] A . Chamblin and G . W . Gibbons, \Topology and Time Reversal," gr-qc/9510006.

[38] E . K . Boyd, S . Ganguli, P . Horava, and U . Varadarajan, \Holographic protection of chronology in universes of the Gödel type," hep-th/0212087.

[39] C . A . R . Herdeiro, \Spinning deformations of the D 1-D 5 system and a geometric resolution of closed timelike curves," hep-th/0212002.

[40] T . Harmark and T . Takayanagi, \Supersymmetric Gödel universes in string theory," hep-th/0301206.

[41] E. G. Gimon and A. Hashimoto, "Black holes in Gödel universes and pp-waves," hep-th/0304181.

[42] L. Dyon, "Chronology protection in string theory," hep-th/0302052.

[43] E. Schrödinger, "Expanding Universes," Cambridge, UK : Univ. Pr. (1956).

[44] G. W. Gibbons, "The Elliptic Interpretation of Black Holes and Quantum Mechanics," Nucl. Phys. B 271 (1986) 497.

[45] N. Sanchez, "Quantum Field Theory and the 'Elliptic Interpretation' of de Sitter Spacetime," Nucl. Phys. B 294 (1987) 1111.

[46] M. K. Parikh, I. Savonije, and E. Verlinde, "Elliptic de Sitter space: dS/Z (2)," Phys. Rev. D 67 (2003) 064005, hep-th/0209120.

[47] A. J. Niemi and G. W. Semenoff, "Finite Temperature Quantum Field Theory in Minkowski Space," Ann. Phys. 152 (1984) 105.

[48] J. S. Schwinger, "Brownian motion of a quantum oscillator," J. Math. Phys. 2 (1961) 407{432.

[49] L. V. Keldysh, "Diagram technique for nonequilibrium processes," Zh. Eksp. Teor. Fiz. 47 (1964) 1515{1527.

[50] N. D. Birrell and P. C. W. Davies, "Quantum Fields in Curved Space," Cambridge Univ. Press (1982).

[51] J. Polchinski, "String theory. Vol. 1: An introduction to the bosonic string," Cambridge Univ. Press (1998).

[52] F. Larsen, A. Naqvi, and S. Terashima, "Rolling tachyons and decaying branes," JHEP 02 (2003) 039, hep-th/0212248.

[53] S. D. Mathur, "Is the Polyakov path integral prescription too restrictive?," hep-th/9306090.

[54] M. B. Green, J. H. Schwarz, and E. Witten, "Superstring Theory. Vol. 1: Introduction," Cambridge Univ. Press (1987).